

Maneuvering Target Tracking Using Multiresolutional Interacting Multiple Model Filter

C. H. Yu*, J. W. Choi**, and T. L. Song***

*School of Mechanical Engineering, Pusan National University, Pusan 609-735, Korea
(Tel: +82-51-510-3203; Fax: +82-51-514-0685; Email:changhoyu@lycos.co.kr)

**School of Mechanical Engineering and Research Institute of Mechanical Technology,
Pusan National University, Pusan 609-735, Korea
(Tel: +82-51-510-2470; Fax: +82-51-514-0685; Email:choijw@pusan.ac.kr)

***Division of Electrical and Computer Engineering, Hanyang University, Ansan 425-791, Korea
(Tel: +82-31-400-5217; Fax: +82-31-407-2756; Email:tsong@hanyang.ac.kr)

Abstract: This paper considers a tracking filter algorithm which can track a maneuvering target. Multiresolutional Interacting Multiple Model (MRIMM) algorithm is proposed to reduce computational burden. In this paper multiresolutional state space model equation and multiresolutional measurement equation are derived by using wavelet transform. This paper shows the outline of MRIMM algorithm. Simulation results show that MRIMM algorithm maintains a good tracking performance and reduces computational burden.

Keywords: Target tracking filter, Interacting multiple model filter, Wavelet transform, Multiresolutional state space model, Multiresolutional measurement.

1. Introduction

Multiresolutional signal processing has been employed in image processing and computer vision to achieve improved performance that cannot be achieved using conventional signal processing techniques at only one resolution level. Multiresolutional estimation with applications to multiresolutional sensor fusion has been investigated by Hong [1]. In [1], measurements are available at each resolution level and the estimates from each level are integrated using the wavelet transform. In this paper the multiresolutional approach is applied to the area of target tracking where measurements are available at only one resolution level. The multiple-model algorithm for tracking maneuvering targets is chosen to demonstrate the effectiveness of the multiresolutional approach and novel results are achieved.

The key ingredients in the multiresolutional approach are multiresolutional modeling and multiresolutional measurements. Although only uniform resolutional measurements are available here, the multiresolutional measurements are calculated by utilizing the wavelet transform [2]. It is true that the calculated measurements at coarser levels do not contain more information than the original measurements. However, when decomposed into lower resolutional levels and due to the effect of "lowpass filtering" of the wavelet transform, the noise is greatly attenuated and the behavior of the maneuver becomes obvious.

The greatest concern regarding the use of wavelet transform related approaches in the target tracking area is the capability of real-time processing. Hong [3] developed a true real-time algorithm. A tree-like data structure was introduced in which the bottom level of the tree corresponded to the highest resolution level and the top level of the tree

represented the coarsest resolution level. The tree was growing and moving as new measurements were acquired and the front branches of the tree were associated with the real-time filtering process.

When a target is in a quiescent motion, the filtering needs not to be performed with maximum process power since the states of a target vary relatively slowly than the time when a target is maneuvering. On the other hand, the measurements process should be performed at as fast rate as possible to maintain the tracking error at some reliable standard or not to lose a track while a target is maneuvering.

In this paper, the MRIMM (multiresolutional interacting multiple model) filter is proposed. When a target is in a quiescent motion, we consider low resolutional measurements by using wavelet transform for computational load saving and consider original resolutional measurements while a target is maneuvering.

2. Discrete wavelet transform

For a sequence of scalar deterministic signals $x(i, n) \in l^2(Z)$, $n \in Z$ at resolution level i , a lower resolution signal can be derived by low-pass filtering with a half-band low-pass filter having an impulse response $h(n)$. A sequence of the lower resolution signal (indicated by an index L) is obtained by downsampling the output of the low-pass filter by two:

$$x_L(i+1, n) = \sum_k h(2n-k)x(i, k) \tag{1}$$

An "added detail" also called wavelet coefficients, which is a complement to $x_L(i+1, n)$ and is denoted $x_H(i+1, n)$, can be computed by first using a high-pass filter with an impulse response $g(n)$ and then downsampling the output of the high-pass filtering by two. The added detailed is given by

$$x_H(i+1, n) = \sum_k g(2n-k)x(i, k) \tag{2}$$

The authors are gratefully acknowledging the financial support by ACRC (Automatic Control Research Center), Seoul National University.

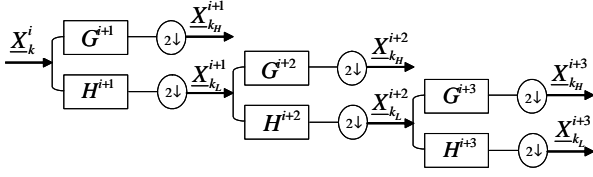


Fig. 1. Sampling and processing rate

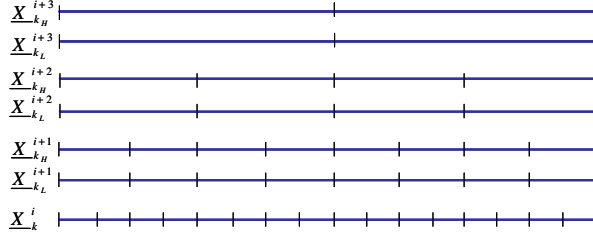


Fig. 2. Sampling and processing rate

The original signal $x(i, n)$ can be recovered from the two filtered and downsampled (lower resolution) signals $x_L(i + 1, n)$ and $x_H(i + 1, n)$. Filters $h(n)$ and $g(n)$ must meet some constraints in order to produce a perfect reconstruction for the signal. In addition to the regularity constraint [4], one constraint is that the filter impulse responses form an orthonormal set. Therefore, (1) and (2) can be considered as a decomposition of the original signal onto an orthonormal basis, and the reconstruction

$$x(i, n) = \sum_k h(2k - n)x_L(i + 1, k) + \sum_k g(2k - n)x_H(i + 1, k) \quad (3)$$

can be considered as a sum of the orthogonal projections. The operation defined by (1) and (2) is called the forward wavelet transform (or wavelet transform for short), and the inverse wavelet transform is described by (3).

The discrete wavelet transform can be implemented by an octave-band filter bank, as shown in Fig. 1 where only three levels are depicted. The dimensions of different decomposed signals at different levels are shown in Fig. 2.

For a sequence of deterministic signals with a finite length, it is more convenient to describe the wavelet transform in an operator form. Consider a sequence of signals at resolution level i with length M :

$$\underline{X}_k^i = \begin{bmatrix} x(i, k - M + 1) \\ x(i, k - M + 2) \\ \vdots \\ x(i, k) \end{bmatrix} \quad (4)$$

The vector form of (1) and (2) can be derived in the following operator form:

$$\underline{X}_{k_L}^{i+1} = H^{i+1} \underline{X}_k^i \quad (5)$$

$$\underline{X}_{k_H}^{i+1} = G^{i+1} \underline{X}_k^i \quad (6)$$

Similarly, when mapping from level $i + 1$ to level i , (3) can also be written in operator form as

$$\underline{X}_k^i = (H^{i+1})^T \underline{X}_{k_L}^{i+1} + (G^{i+1})^T \underline{X}_{k_H}^{i+1} \quad (7)$$

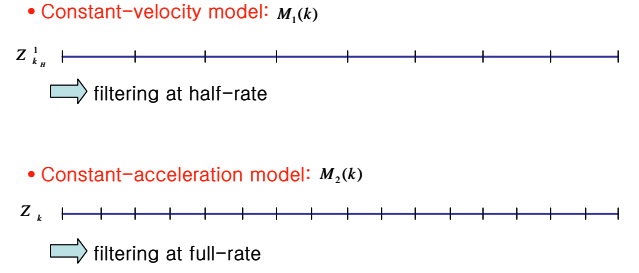


Fig. 3. Sampling and processing rate

where $()^T$ is the matrix transpose operation.

A simultaneous multilevel signal decomposition can be carried out by a filter bank. For instance, to decompose \underline{X}_k^i into three levels, as shown in Fig. 2, the following decomposition transform can be applied:

$$\begin{bmatrix} \underline{X}_{k_L}^{i+3} \\ \underline{X}_{k_H}^{i+3} \\ \underline{X}_{k_H}^{i+2} \\ \underline{X}_{k_H}^{i+1} \end{bmatrix} = T^{i+3|i} \underline{X}_k^i \quad (8)$$

where

$$T^{i+3|i} = \begin{bmatrix} H^{i+3} H^{i+2} H^{i+1} \\ G^{i+3} H^{i+2} H^{i+1} \\ G^{i+2} H^{i+1} \\ G^{i+1} \end{bmatrix} \quad (9)$$

is an orthogonal matrix mapping \underline{X}_k^i onto three levels of the filter bank simultaneously.

3. MRIMM filter

The conventional IMM (interacting multiple model) filter [5] has been implemented using models of different dimension, a second-order model for the quiescent model of the target and one or two third-order models for the maneuvering mode with different process noise levels. The approach consists of running a filter for each model, a model probability evaluator, and an estimate combiner at the output of the filters. Each filter uses a mixed estimate at the beginning of each cycle.

While the IMM filter uses full-rate filtering, MRIMM filter uses both full-rate and half-rate filtering. In MRIMM filter, one sub-filter for constant velocity model uses half-rate measurements by using wavelet transform to reduce a computational load, other sub-filter for constant acceleration model uses full-rate measurements, as shown in Fig. 3. And the initial value at each sampling time can be achieved as shown in Fig. 4.

And one cycle of the MRIMM filter consists of 4 steps such as interacting step, Kalman filtering, calculating the model probability, and combining the estimates of the each sub-filters.

3.1. Multiresolutional measurements and models

The system with a high rate si given by

$$x(i, k + 1) = Ax(i, k) + w(i, k) \quad (10)$$

$$z(i, k) = Cx(i, k) + v(i, k) \quad (11)$$

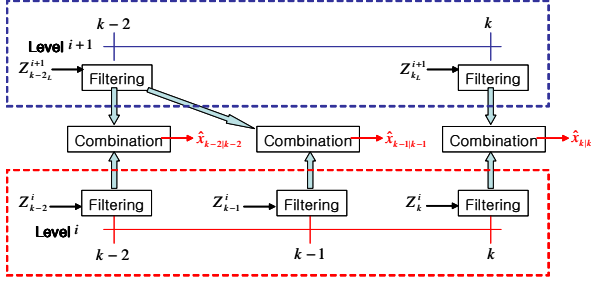


Fig. 4. Sampling and processing rate

where

$$E[w(i, k)] = 0, \quad E[w(i, k)w(i, k)^T] = Q(i, k) \quad (12)$$

$$E[v(i, k)] = 0, \quad E[v(i, k)v(i, k)^T] = R(i, k) \quad (13)$$

$$E[v(i, k)w(i, k)] = 0 \quad (14)$$

A set of different low rate models can be derived recursively from the high rate model given in Eqs. (10) and (11). To simplify the discussion, in the following we will use two-tap Harr filter. The first-level lowpass filtered measurement $z_L(i+1, k)$ is derived by

$$z_L(i+1, k) = h_1 z(i, k-1) + h_2 z(i, k) \quad (15)$$

where $[h_1 \ h_2] = H$ is a two-tap Haar lowpass filter. Substituting measurement model (11) into Eq. (15) results in a first-level low rate model for lowpass filtered measurements

$$z_L(i+1, k) = C^1 x_L(i+1, k) + v_L(i+1, k) \quad (16)$$

where

$$x_L(i+1, k) = h_1 x(i, k-1) + h_2 x(i, k) \quad (17)$$

$$C^1 = C \quad (18)$$

and

$$v_L(i+1, k) = h_1 v(i, k-1) + h_2 v(i, k) \quad (19)$$

with

$$E[v_L(i+1, k)] = 0 \quad (20)$$

$$\begin{aligned} R_L(i+1, k) &= [v_L(i+1, k)v_L(i+1, k)^T] \\ &= h_1^2 R(i, k-1) + h_2^2 R(i, k) \end{aligned} \quad (21)$$

The first-level low rate system model is

$$x_L(i+1, k+1) = A^1 x_L(i+1, k) + w_L(i+1, k) \quad (22)$$

where

$$A^1 = (A)^2 \quad (23)$$

and

$$E[w_L(i+1, k)] = 0 \quad (24)$$

$$\begin{aligned} Q_L(i+1, k) &= [w_L(i+1, k)w_L(i+1, k)^T] \\ &= h_1^2 A Q(i, k-1) A^T \\ &\quad + (h_1 I + h_2 A) Q(i, k) (h_1 I + h_2 A)^T \\ &\quad + h_2^2 Q(i, k+1) \end{aligned} \quad (25)$$

The other level low rate models can be derived recursively as

$$x_L(j, k+1) = A^j x_L(j, k) + w_L(j, k) \quad (26)$$

$$z_L(j, k) = C^j x_L(j, k) + v_L(j, k) \quad (27)$$

where

$$A^j = (A^{j-1})^2 \quad (28)$$

$$C^j = C^{j-1} \quad (29)$$

The noise statistics of $w_L(j, k)$ and $v_L(j, k)$ are derives as

$$E[w_L(j, k)] = 0 \quad (30)$$

$$\begin{aligned} Q_L(j, k) &= E[w_L(j, k)w_L(j, k)^T] \\ &= h_1^2 A^{j-1} Q_L(j-1, k-1) (A^{j-1})^T \\ &\quad + (h_1 I + h_2 A^{j-1}) Q_L(j-1, k) (h_1 I + h_2 A^{j-1})^T \\ &\quad + h_2^2 Q_L(j-1, k+1) \end{aligned} \quad (31)$$

and

$$E[v_L(j, k)] = 0 \quad (32)$$

$$\begin{aligned} R_L(j, k) &= E[v_L(j, k)v_L(j, k)^T] \\ &= h_1^2 R_L(j-1, k-1) + h_2^2 R_L(j-1, k) \end{aligned} \quad (33)$$

3.2. Interacting step

Initial estimate can be derived by

$$\begin{aligned} \hat{x}_t(k-1|k-1)_{ini} &= E[x(k-1)|M_t(k), Z^{k-1}] \\ &= \sum_{s=1}^N E[x(k-1)|M_s(k-1), Z^{k-1}] \\ &\quad \times p[M_s(k-1)|M_t(k), Z^{k-1}] \end{aligned} \quad (34)$$

where as $x(k-1)$ is independent from $M_t(k)$, following eq. can be derived.

$$\begin{aligned} \hat{x}_t(k-1|k-1)_{ini} &= \sum_{s=1}^N \hat{x}_s(k-1|k-1) \\ &\quad \times p[M_s(k-1)|M_t(k), Z^{k-1}] \\ &= \sum_{s=1}^N \hat{x}_s(k-1|k-1) \mu_{s|t}(k-1|k-1) \end{aligned} \quad (35)$$

where $\mu_{s|t}$ can be calculated as

$$\begin{aligned} \mu_{s|t}(k-1|k-1) &= p[M_s(k-1)|M_t(k), Z^{k-1}] \\ &= p[M_t(k)|M_s(k-1), Z^{k-1}] \\ &\quad \times \frac{p[M_s(k-1)|Z^{k-1}]}{p[M_t(k)|Z^{k-1}]} \end{aligned} \quad (36)$$

Substituting Eq. (36) into Eq. (35) results in an initial estimate

$$\begin{aligned} \hat{x}_t(k-1|k-1)_{ini} &= \sum_{s=1}^N \hat{x}_s(k-1|k-1) \\ &\times p[M_t(k)|M_s(k-1), Z^{k-1}] \\ &\times \frac{p[M_s(k-1)|Z^{k-1}]}{p[M_t(k)|Z^{k-1}]} \end{aligned} \quad (37)$$

Similarly, an initial error covariance matrix can be derived as

$$\begin{aligned} P_t(k-1|k-1)_{ini} &= \sum_{s=1}^N \mu_{s|t}(k-1|k-1) \\ &\times \{P_s(k-1|k-1) \\ &+ [\hat{x}_s(k-1|k-1) - \hat{x}_t(k-1|k-1)_{ini}] \\ &\times [\hat{x}_s(k-1|k-1) - \hat{x}_t(k-1|k-1)_{ini}]^T\} \end{aligned} \quad (38)$$

3.3. Kalman filtering

First, one cycle of the Kalman filter for state and covariance estimation for the constant acceleration model is in the following.

$$\hat{x}_t(k|k-1) = A\hat{x}_t(k-1|k-1) \quad (39)$$

$$P_t(k|k-1) = AP_t(k-1|k-1)A^T + Q(k) \quad (40)$$

$$\hat{x}_t(k|k) = \hat{x}_t(k|k-1) + G_t(k)r_t(k) \quad (41)$$

$$P_t(k|k) = [I - G_t(k)C]P_t(k-1|k-1) \quad (42)$$

$$r_t(k) = z(k) - C\hat{x}_t(k|k-1) \quad (43)$$

$$S_t(k) = CP_t(k|k-1)C^T + R(k) \quad (44)$$

$$G_t(k) = P_t(k|k-1)C^T S_t(k)^{-1} \quad (45)$$

where, $r_t(k)$ is the residual, $S_t(k)$ is the covariance for the residual, $G_t(k)$ is the filter gain.

And one cycle of the Kalman filter for the constant velocity model is in the following.

$$\hat{x}_L(2, k|k-1) = A^1 \hat{x}_L(2, k-1|k-1) \quad (46)$$

$$P_L(2, k|k-1) = A^1 P_L(2, k-1|k-1)(A^1)^T + Q_L(2, k) \quad (47)$$

$$\hat{x}_L(2, k|k) = \hat{x}_L(2, k|k-1) + G_L(2, k)r_L(2, k) \quad (48)$$

$$P_L(2, k|k) = [I - G_L(2, k)C^1]P_L(2, k-1|k-1) \quad (49)$$

$$r_L(2, k) = z_L(2, k) - C^1 \hat{x}_L(2, k|k-1) \quad (50)$$

$$S_L(2, k) = C^1 P_L(2, k|k-1)(C^1)^T + R_L(2, k) \quad (51)$$

$$G_L(2, k) = P_L(2, k|k-1)(C^1)^T S_L(2, k)^{-1} \quad (52)$$

3.4. Calculating the model probability

A model probability $\mu_t(k)$ of the target can be derived by following Eq.

$$\begin{aligned} \mu_t(k) &= p[M_t(k)|Z^k] \\ &= p[M_t(k)|z(k), Z^{k-1}] \\ &= \frac{p[z(k)|M_t(k), Z^{k-1}]p[M_t(k)|Z^{k-1}]}{p[z(k)|Z^{k-1}]} \\ &= p[z(k)|M_t(k), Z^{k-1}] \\ &\times \sum_{s=1}^N p[M_t(k)|M_s(k-1), Z^{k-1}] \\ &\times \frac{p[M_s(k-1)|Z^{k-1}]}{p[z(k)|Z^{k-1}]} \end{aligned} \quad (53)$$

3.5. Combining the estimates

The estimate at every sampling time from each sub-filters is derived as

$$\begin{aligned} \hat{x}(2k|2k) &= \hat{x}_1(2, 2k|2k-1)[1 - \mu_2(2k)] \\ &+ \hat{x}_2(2k|2k)\mu_2(2k) \end{aligned} \quad (54)$$

$$\begin{aligned} P(2k|2k) &= [1 - \mu_2(2k)] \\ &\times \{P_1(2, 2k|2k-1) + [\hat{x}_1(2, 2k|2k-1) - \hat{x}(2k|2k)] \\ &\times [\hat{x}_1(2, 2k|2k-1) - \hat{x}(2k|2k)]^T\} \\ &+ \mu_2(2k) \\ &\times \{P_2(2k|2k) + [\hat{x}_2(2k|2k) - \hat{x}(2k|2k)] \\ &\times [\hat{x}_2(2k|2k) - \hat{x}(2k|2k)]^T\} \end{aligned} \quad (55)$$

$$\begin{aligned} P(2k+1|2k+1) &= [1 - \mu_2(2k+1)] \{P_1(2, 2k|2k-1) \\ &+ [\hat{x}_1(2, 2k+1|2k+1) - \hat{x}(2k+1|2k+1)] \\ &\times [\hat{x}_1(2, 2k+1|2k+1) - \hat{x}(2k+1|2k+1)]^T\} \\ &+ \mu_2(2k+1) \{P_2(2k|2k-1) \\ &+ [\hat{x}_2(2k+1|2k+1) - \hat{x}(2k+1|2k+1)] \\ &\times [\hat{x}_2(2k+1|2k+1) - \hat{x}(2k+1|2k+1)]^T\} \end{aligned} \quad (56)$$

4. Simulation results

This section highlights some of the results of a Monte Carlo comparison between the IMM and MRIMM algorithms.

4.1. Target scenario and parameter configuration

Initial position of the target is $0m$ and initial velocity is $-250m/sec$, and initial acceleration is $0m/sec^2$. Maneuver of $20m/sec^2$ occurs between $30sec$ and $60sec$. Sampling time is set to $1sec$.

Process noise variances are set to $q_c^2(k) = 2^2 m^2/sec^4$ and $q_m^2(k) = 3^2 m^2/sec^4$, and measurement noise covariance is set to $12^2 m^2$. And model transition probability is set to

$$p_{jump} = \begin{bmatrix} 0.85 & 0.15 \\ 0.15 & 0.85 \end{bmatrix} \quad (57)$$

4.2. Comparative results

Fig. 5 shows a RMS estimate position error. As shown in Fig. 5, the estimate error of MRIMM is similar to the estimate of conventional IMM. However, Table 1 shows that the computational load of MRIMM is lower than the IMM by 20

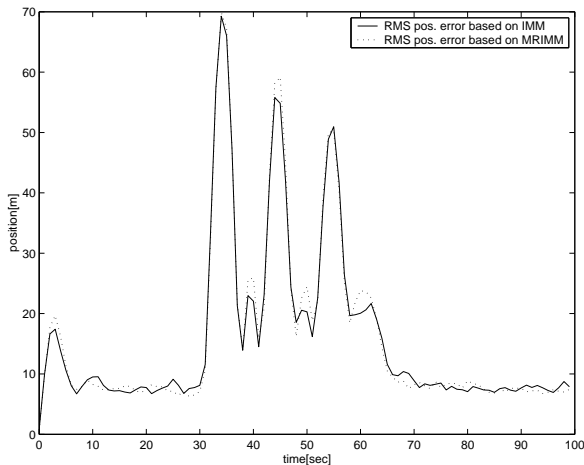


Fig. 5. Sampling and processing rate

Table 1. Computational load

	IMM	MRIMM
Flops	5,291,193	4,232,954
Percentage	100%	80%

5. Conclusions

In this paper, a theoretical foundation for MRIMM target tracking is established. Based on the discrete wavelet transform, a set of multiresolutional models has been developed which make the MRIMM possible. The algorithm, in general, outperforms the full-rate IMM for nonmaneuvering targets and performs comparably for maneuvering targets. Computational savings are achieved.

References

- [1] Hong, L., "Multiresolutional estimation using wavelet transform," *IEEE Transactions on Aerospace and Electronic Systems*, vol. 29, no. 4, pp. 1244-1251, 1993.
- [2] Mallat, S. G., "A theory for multiresolution signal decomposition: The wavelet representation," *IEEE Transactions on Pattern Analysis and Machine Intelligence*, vol. 11, no. 7, pp. 674-693, 1989.
- [3] Hong, L., and Scaggs, T., "Real-time optimal filtering for stochastic systems with multiresolutional measurements," *Systems Control Letters*, vol. 20, pp. 381-387, 1993.
- [4] Daubechies, I., "Orthonormal bases of compact supported wavelets," *Communications on Pure and Applied Mathematics*, XLI, pp. 909-996, 1988.
- [5] Blom, H. A. P., and Bar-Shalom, Y., "The interacting multiple model algorithm for systems with Markovian switching coefficients," *IEEE Trans. on Automatic Control*, vol. AC-33, no. 8, pp. 780-783, August 1998.